International Journal of Nanomedicine

Dovepress
open access to scientific and medical research

Open Access Full Text Article

ORIGINAL RESEARCH

Pluronic® P123/F127 mixed micelles delivering sorafenib and its combination with verteporfin in cancer cells

This article was published in the following Dove Press journal:
International Journal of Nanomedicine
6 September 2016
Number of times this article has been viewed

Diogo Silva Pellosi[1,2,*]
Francesca Moret[3,*]
Aurore Fraix[4]
Nino Marino[4]
Sara Maiolino[2]
Elisa Gaio[3]
Noboru Hioka[1]
Elena Reddi[3]
Salvatore Sortino[4]
Fabiana Quaglia[2]

[1]Research Nucleus of Photodynamic Therapy, Chemistry Department, State University of Maringá, Maringá, Brazil; [2]Drug Delivery Laboratory, Department of Pharmacy, University of Naples Federico II, Naples, [3]Cell Biology Unit, Department of Biology, University of Padova, Padua, [4]Laboratory of Photochemistry, Department of Drug Sciences, University of Catania, Catania, Italy

*These authors contributed equally to this work

Abstract: Here, we developed Pluronic® P123/F127 (poloxamer) mixed micelles for the intravenous delivery of the anticancer drug sorafenib (SRB) or its combination with verteporfin (VP), a photosensitizer for photodynamic therapy that should complement well the cytotoxicity profile of the chemotherapeutic. SRB loading inside the core of micelles was governed by the drug:poloxamer weight ratio, while in the case of the SRB–VP combination, a mutual interference between the two drugs occurred and only specific ratios could ensure maximum loading efficiency. Coentrapment of SRB did not alter the photophysical properties of VP, confirming that SRB did not participate in any bimolecular process with the photosensitizer. Fluorescence resonance energy-transfer measurement of micelles in serum protein-containing cell-culture medium demonstrated the excellent stability of the system in physiologically relevant conditions. These results were in line with the results of the release study showing a release rate of both drugs in the presence of proteins slower than in phosphate buffer. SRB release was sustained, while VP remained substantially entrapped in the micelle core. Cytotoxicity studies in MDA-MB231 cells revealed that at 24 hours, SRB-loaded micelles were more active than free SRB only at very low SRB concentrations, while at 24+24 hours a prolonged cytotoxic effect of SRB-loaded micelles was observed, very likely mediated by the block in the S phase of the cell cycle. The combination of SRB with VP under light exposure was less cytotoxic than both the free combination and VP-loaded micelles + SRB-loaded micelles combination. This behavior was clearly explainable in terms of micelle uptake and intracellular localization. Besides the clear advantage of delivering SRB in poloxamer micelles, our results provide a clear example that each photochemotherapeutic combination needs detailed investigations on their particular interaction, and no generalization on enhanced cytotoxic effects should be derived a priori.

Keywords: Pluronic® micelles, sorafenib, chemotherapy, photodynamic therapy, verteporfin

Introduction

Nanotechnologies promise to refine cancer treatments in trying to overcome several issues associated with conventional chemotherapy by improving treatment efficacy, decreasing systemic side effects, and overcoming multidrug resistance. In the wide scenario of nanoplatforms available for anticancer drug delivery, polymeric micelles based on biocompatible polymers have been attracting interest, due to great versatility, small size, ease of functionalization, and potential to transport a multidrug cargo for combination therapies.[1–3] Representatives of such materials are Pluronic® (poloxamer) copolymers, which are surfactant molecules containing two hydrophilic poly(ethylene oxide) (PEO) and one hydrophobic poly(propylene oxide) (PPO) regions arranged in a PEO–PPO–PEO triblock

Correspondence: Salvatore Sortino
Laboratory of Photochemistry, Department of Drug Sciences, University of Catania, 6 Viale Andrea Doria, Catania I-95125, Italy
Tel +39 095 738 5079
Fax +39 095 580 138
Email ssortino@unict.it

submit your manuscript | www.dovepress.com
Dovepress
http://dx.doi.org/10.2147/IJN.S103344

structure. In water, poloxamer copolymers self-assemble in core–shell nanosize micelles and entrap poorly water-soluble drugs, increasing their apparent solubility. Furthermore, drug-loaded poloxamer micelles can passively target tumors by the enhanced permeability and retention (EPR) effect after intravenous injection. Poloxamer unimers have also shown the ability to hypersensitize multidrug-resistant cells by inhibiting glycoprotein P-mediated drug efflux.[4,5]

Mixed micelles made of more than one type of Pluronic®, a registered trademark of BASF, manifest properties superior to those made of the individual components. In fact, the correct selection of poloxamer type and unimer ratio induces a synergistic aggregation thus producing micelles with improved characteristics in term of colloidal stability and drug loading efficiency.[6]

For example, in a very recent paper, we demonstrated that poloxamer mixed micelles enhanced the solubility and photodynamic activity of very hydrophobic benzoporphyrin derivatives.[7]

Sorafenib (SRB) is a drug approved for the treatment of advanced inoperable hepatocellular and advanced renal cancers after oral administration (Nexavar®).[8,9] Its possible use for systemic treatment of liver fibrosis[10] and hepatocellular carcinoma[11–13] has been recently highlighted. SRB is an inhibitor of different Raf serine/threonine kinase isoforms mediating cell proliferation, and blocks upstream receptor tyrosine kinases, which play an important role in angiogenesis.[14]

Angiogenesis and tumor revascularization due to VEGF expression is a major problem associated with photodynamic therapy (PDT) application in cancer.[15] Indeed, PDT is a therapeutic procedure that uses a light-activated photosensitizer (PS) to produce reactive oxygen species, especially singlet oxygen ($^1O_2$), which trigger the destruction of tumor cells, damage to tumor vasculature, and a severe inflammatory action.[16,17] Coadministration of PDT agents with antiangiogenic chemotherapeutics could be a promising strategy to potentiate photodynamic treatments. Verteporfin (VP) is a US Food and Drug Administration clinically approved agent for PDT of age-related macular degeneration (Visudyne®) and is currently in Phase I/II clinical trials to treat locally advanced pancreatic cancer.[18] It was found that VP induced angiogenesis in the chicken chorioallantoic membrane model could be inhibited by SRB, giving prolonged vascular occlusion in the treated areas due to a synergistic effect.[19]

Since the entrapment of multiple therapeutic agents in a single nanocarrier allows precise and controlled delivery of the optimal drug ratio in the same area of the body, enormous clinical advantages can be brought about.[3,20,21] Currently, this novel "two-in-one" approach is under clinical and preclinical investigation against several cancer types.[22,23] Furthermore, delivery in a nanocarrier can also alleviate poor water solubility, a drawback shared by several chemotherapeutics and PS. Although very promising in principle, there have been very few attempts in developing poloxamer micelles for the codelivery of PS and other anticancer molecules.[24,25]

In this contribution, we aim to explore the potential of poloxamer mixed micelles as a suitable intravenous nanocarrier to deliver SRB while maintaining its activity and mechanism of action. Besides, we also focus on the combined delivery of SRB and VP, investigating how it can affect single-drug cytotoxicity. To this end, poloxamer micelles were loaded with SRB alone or in combination with VP. Drug-loading efficiency and -release rate, spectroscopic and photodynamic properties of the micelles, and stability in complex media were assessed. Finally, the cytotoxicity of SRB and its combination with VP and trafficking of micelles in MDA MB-231 breast carcinoma cells were investigated.

Materials and methods

Materials

SRB free base (molecular weight [MW] 464.8 g·mol^{-1}) was purchased from LC Laboratories, a division of PKC Pharmaceuticals Inc (Woburn, MA, USA). VP (benzoporphyrin-derivative monoacid ring A, MW 718.8 g·mol^{-1}) was kindly supplied by Professor D Dolphin (University of British Columbia, Vancouver, BC, Canada). Poloxamer P123 (EO_{20}–PO_{65}–EO_{20}, MW 5,750 g·mol^{-1}), poloxamer F127 (EO_{100}–PO_{65}–EO_{100}, MW 12,600 g·mol^{-1}), trehalose, polysorbate 80, and Nile red (NR) were purchased from Sigma-Aldrich. Ethanol, dichloromethane, diethyl ether, acetone, and acetonitrile were purchased from Carlo Erba Reagents. All the other chemicals were of analytical reagent grade and used without previous purification.

Preparation of drug-loaded micelles

Unloaded, SRB, and SRB–VP-loaded poloxamer micelles were prepared by the thin-film hydration method.[26] Briefly, 10 mg of poloxamer mixture (proportion 2:1 w:w, which corresponded to 3.33 mg of F127 and 6.67 mg of P123) was dissolved in 1 mL of ethanol in a round-bottom flask. For drug-loaded micelles, different amounts of SRB (100–200 µg) and VP (4–10 µg) were dissolved in 1 mL ethanol and added to the poloxamer solution. Then, the solvent was evaporated by rotary evaporation at 50°C for approximately 20 minutes. Residual solvent in the film was removed under vacuum overnight. After that, the dried film was hydrated with 1 mL of filtered distilled water under sonication

for 5 minutes to obtain a limpid solution and filtered through 0.22 μm Phenex(R)-RC filters (Phenomenex, Torrance, CA, USA) to remove the unloaded drug or possible large cylindrical aggregates formed by P123. When necessary, the resulting solution was lyophilized for 24 hours in the presence of trehalose (2:1 mass ratio with the copolymer).

Micelle characterization

Hydrodynamic diameter (D_H), polydispersity index (PI), and ζ-potential of micelles were determined using a Zetasizer Nano ZS (Malvern Instruments Ltd, Malvern, UK). The freeze-dried formulations were dispersed in Milli-Q water and measurements were performed at 37°C at a 90° angle. Results are reported as mean values of three separated measurements on three different micelle batches ± standard deviation (SD).

SRB- and VP-entrapment efficiency

SRB- and VP-encapsulation efficiency was evaluated by dissolving a known amount of freeze-dried micelles (10 mg) in 1 mL of ethanol. Before the analysis, the sample was filtered through a 0.22 μm filter (A Chemtek). Results are reported as mean values of three separated measurements of three different samples ± SD.

SRB was analyzed by high-performance liquid chromatography on a Shimadzu apparatus equipped with an LC-10ADvp pump, an SPD-10Avp ultraviolet-visible (UV-vis) detector and a C-R6 integrator. The analysis was performed on a SphereClone ODS 25 μm, C18 column (250×4.6 mm, 80 Å) (Phenomenex, Torrance, CA, USA). The mobile phase was a 35:65 (v:v) mixture of water and acetonitrile pumped at a flow rate of 1 mL/min. The water phase contained triethylamine (2% v:v), and was adjusted to pH 5.4 with phosphoric acid. The UV detector was set at 265 nm. A calibration curve for SRB in ethanol was constructed in the concentration range 0.002–0.2 mg/mL. To exclude possible interference of VP on SRB quantitative analysis, an amount of VP-loaded micelles was dissolved in ethanol and analyzed in the same conditions.

VP quantification was carried out by spectrophotometry on a Shimadzu UV-1800. The concentration of VP was calculated by means of a standard calibration curve derived for ethanol solutions of VP at known concentrations (20–0.1 μg/mL). Potential interference of SRB on absorption was preliminarily assessed by spiking a VP solution in ethanol with different amounts of SRB.

Absorption, emission, and transient spectroscopy

UV-vis absorption and fluorescence spectra were recorded with a Jasco V-560 spectrophotometer and Fluorolog-2 (F-111) spectrofluorometer, respectively. All measurements were performed in a thermostated quartz cell (1 cm path length, 3 mL capacity).

Steady-state emission of $^1O_2$ was recorded in D_2O solutions with a Fluorolog-2 111 spectrometer, equipped with an InGaAs detector maintained at −196°C, by illuminating orthogonally the sample at 405 nm with a continuous-wave laser. For laser-flash photolysis, all the samples were excited with the second harmonic of Nd:YAG Continuum Surelite II-10 laser (532 nm, 6 ns full width at half maximum), using quartz cells with a path length of 1 cm. The excited solutions were analyzed with a Luzchem Research mLFP-111 apparatus with an orthogonal pump/probe configuration. The probe source was a ceramic xenon lamp coupled to quartz fiber-optic cables. The laser pulse and the mLFP-111 system were synchronized by a Tektronix TDS 3032 digitizer, operating in pretrigger mode. The signals from a compact Hamamatsu photomultiplier were initially captured by the digitizer and then transferred to a personal computer, controlled by Luzchem Research software operating in the National Instruments LabView 5.1 environment. The solutions were deoxygenated by bubbling with a vigorous and constant flux of pure argon (previously saturated with solvent). In all of these experiments, the solutions were renewed after each laser shot (in a flow cell of 1 cm optical path), to prevent probable auto-oxidation processes. The sample temperature was 295±2 K. The energy of the laser pulse was measured at each shot with an SPHD25 Scientech pyroelectric meter.

Micelle behavior in cell-culture medium

Micelle stability in the medium employed for cell studies (Dulbecco's Modified Eagle's Medium [DMEM] enriched with 10% fetal bovine serum [FBS]) was evaluated. Briefly, 20 mg of micelles was added to 2 mL of cell-culture medium and incubated at 37°C for 72 hours. At selected time intervals, size and ζ-potential were evaluated. Micelle stability was also evaluated by fluorescence resonance energy transfer (FRET) by coencapsulating two different fluorescence probes into a micelle core.[27] The hydrophobic dye NR was chosen as the fluorescent donor and VP as the acceptor molecule. VP–NR micelles were prepared as described earlier for SRB–VP micelles. The concentration of NR in the micelles was 0.8 $\mu g \cdot mL^{-1}$ and that of VP 4 $\mu g \cdot mL^{-1}$, which gave a VP:NR ratio of 5:1 by weight. The ratio between the maximum intensity of emission bands for VP and NR was monitored as function of time. Decrease of this ratio and/or micelle-size increase was considered indicative of micelle aggregation or disassembly in cell-culture medium. DMEM without FBS was also evaluated as a control experiment. Results

are reported as mean values of three separate measurements (n=3) ± SD.

For release studies in phosphate-buffered saline (PBS) or in cell-culture medium, the formulation (10 mg of poloxamer; SRB =100 μg·mL^{-1} and VP =10 μg·mL^{-1}) was dispersed in 1 mL of DMEM with 10% FBS and placed in a dialysis bag (MW cutoff 3,500 Da, Spectra/Por®). The sample was plunged in 5 mL of PBS containing 5% v:v of polysorbate 80 (sink condition) and kept at 37°C up to 72 hours. At selected time intervals, 1 mL of release medium was withdrawn and replaced with an equal volume of fresh medium. SRB and VP quantitative analyses were carried out as described earlier. As control, release profiles of free drugs diluted in PBS or DMEM with 10% FBS medium are reported for comparison. Results are expressed as release percentage over time (n=3) ± SD.

In vitro experiments

Cell culture

The human breast cancer cell line MDA-MB231 was purchased from the American Type Culture Collection (Manassas, VA, USA). The cells were grown in DMEM with GlutaMax™ supplemented with 10% FBS, 100 U/mL, streptomycin and 100 μg/mL penicillin G (Thermo Fisher Scientific, Waltham, MA, USA), and maintained at 37°C in a humidified atmosphere containing 5% CO_2.

Dark and phototoxicity (PDT) in vitro

The cytotoxicity in the dark of MDA-MB231 cells incubated with VP, SRB, and their combination (free or loaded in poloxamer micelles) was measured with the MTS (3-[4,5-dimethylthiazol-2-yl]-5-[3-carboxymethoxyphenyl]-2-[4-sulfophenyl]-2*H*-tetrazolium) assay after 24 hours of incubation, as well as after an additional 24 hours of cell growth in drug-free medium. Cells (6×10^3) were seeded in 96-well plates (24 hours of growth) and then incubated with the drug formulations for 24 or 24+24 hours. Lyophilized formulations containing 10 mg of micelles (loaded with 10 μg of VP and/or 100 μg of SRB) were solubilized in 2 mL DMEM and then further diluted in medium added with 10% FBS. For the MTS assay, the medium was replaced with 100 μL of serum-free medium and 20 μL of CellTiter 96® Reagent (Promega Corporation, Fitchburg, WI, USA) and the wells incubated for 1 hour at 37°C. Absorbance at 492 nm was measured with a Multiskan Go (Thermo Fischer Scientific) plate reader, and the viability of treated cells was expressed as a percentage of the absorbance of control cells that was taken as 100% viability. For the in vitro PDT experiments, cells were seeded as described earlier. After 24 hours of incubation with the different drug formulations, the cells were washed once with PBS with Ca^{2+} and Mg^{2+}, and irradiated in PBS with 0.75 J·cm^{-2} of red light (600–700 nm, fluence rate 25 mW·cm^{-2}) from a PDT 1200 lamp (Herbert Waldmann GmbH & Co KG, Villingen-Schwenningen, Germany). Immediately after irradiation, the cells were brought back to the incubator after replacement of PBS with fresh medium. Cell viability was measured with the MTS test after an additional 24 hours.

Cellular uptake studies

Cells (5×10^4) were grown in 24-well plates for 24 hours and incubated for 24 hours with increasing concentrations of free VP, VP-loaded micelles, or VP–SRB-loaded micelles diluted in cell medium added with 10% FBS. After incubation, the cells were washed twice with Versene™ and detached from the plates with trypsin, which was neutralized by the addition of FBS. Cells were centrifuged and resuspended in Versene before VP fluorescence was measured by a FACSCanto™ II (BD Biosciences, San Jose, CA, USA) flow cytometer. The blue laser at 488 nm was used as the excitation source, and wavelengths of 670–735 nm (PerCP channel) were selected for the detection of VP fluorescence. A total of 10^5 events/sample were acquired and analyzed with FACSDiva software.

Cell-cycle analysis

Cells (10^6) were seeded in 100 mm culture dishes and incubated with 10 μM SRB free or loaded in poloxamer micelles for 24 or 24+24 hours. Treated and control cells were harvested, fixed in 70% cold ethanol, and stored overnight at 4°C. Before analysis, cells were washed in distilled water, centrifuged, and resuspended in 1 mL PBS containing 50 μg/mL propidium iodide (Sigma-Aldrich) and 100 μg/mL ribonuclease for DNA staining. Samples were incubated for 1 hour at 37°C and then analyzed by flow cytometry. Data from 2×10^4 cells/sample were acquired with the FACSDiva software and analyzed with ModFit LT 3.0 software (BD Biosciences) to determine alterations in cell-cycle distribution.

Confocal microscopy

The intracellular localization of VP, free or loaded in poloxamer micelles, was determined by confocal microscopy. Cells (8×10^4), seeded in special tissue-culture dishes for fluorescence microscopy (μ-Dish 35mm, high; Ibidi GmbH, Planneg, Germany), were allowed to grow for 24 hours and

then incubated for 24 hours. Fifteen minutes before the end of the incubation, the cells were stained with MitoTracker® green FM (100 nM) or ER-Tracker green (1 μM), used as markers for mitochondria and endoplasmic reticulum, respectively. Cells were then washed twice with Hanks's balanced salt solution and analyzed with an SP5 confocal laser-scanning microscope (Leica Microsystems, Wetzlar, Germany); the images were elaborated with ImageJ software.

Statistical analysis

Primer software for biostatistics (McGraw-Hill, New York, NY, USA) was used for statistical analysis of the data. The data are expressed as mean values ± SD for at least three independent experiments. The difference between groups was evaluated with Student's *t*-test or with the Bonferroni test, and was considered significant at $P<0.05$.

Results and discussion

Properties of drug-loaded micelles

A preliminary study was devoted to evaluate the optimal conditions to obtain micelles with good encapsulation efficiencies of SRB alone and in combination with VP. In a previous work, we demonstrated that the thin-film method followed by freeze-drying (with trehalose as cryoprotectant) allows preparation of poloxamer mixed micelles loaded with VP.[7] Results of this previous study demonstrated that the optimal ratio between P123 and F127 was at 2:1 (w:w). This ratio was maintained in micelles explored here. Table 1 summarizes the physicochemical characteristics and drug-loading parameters of poloxamer micelles loaded with SRB (and SRB–VP combination).

The D_H of empty and drug-loaded micelles demonstrated that poloxamer form micelles with a size ranging between 25 and 43 nm and satisfactory PI. SRB entrapment was very efficient: up to 2% drug:polymer by weight without any change in terms of size or PI. Loading a combination of SRB and VP was feasible, and mainly controlled by the initial amount of SRB employed, which is the most abundant drug in formulations. Considering that both drugs have low water solubility, it can be reasonably hypothesized that when entrapped together, a mutual interference in the micelle core may occur. As generally observed for polymeric micelles, the drug:poloxamer ratio was found to be a critical parameter to control encapsulation efficiency.[28] In fact, the lipophilic drugs accommodate inside the PPO core of poloxamer mixed micelles, and once these domains are saturated, a decrease in encapsulation efficiency is experienced.[29] The size increase after entrapment of the drug combination can be ascribed to an increase in PPO core size, probably due to the presence of entangled drugs. Nevertheless, the micelles were still small enough for tumor-specific accumulation via the EPR effect.[4] Therefore, optimal encapsulation efficiencies were found at 100 $\mu g \cdot mL^{-1}$ for SRB and 4 $\mu g \cdot mL^{-1}$ for VP. Under this condition, both loading values can be considered satisfactory for a therapeutically relevant system. All formulations presented slightly negative ζ-potential values, as generally found for polyethylene glycolated nanocarriers made of uncharged polymers.

Thin-film rehydration provided a fluffy lyophilized product, readily reconstituted in water within 20–30 seconds of manual shaking, as already demonstrated in our previous work.[7] The storage stability of the lyophilized formulations (Figure S1) demonstrated a small decrease in drug content, with a slight size increase (~5–6 nm) after reconstitution of

Table 1 Composition and properties of Pluronic® (poloxamer) P123/F127 2:1 w:w mixed micelles encapsulating SRB and SRB–VP combination

SRB (μg)	VP (μg)	SRB loading[a] (EE%)[b]	VP loading[a] (EE%)[b]	Mean D_H (nm)	PI	ζ-potential (mV)
–	–	–	–	25.3±1.8	0.162	–4.37±0.96
–	4	–	0.038±0.002 (95.3±1.7)	26.3±1.8	0.18	–6.69±0.78
–	6	–	0.053±0.004 (89.2±2.4)	30.6±2.7	0.223	–5.27±1.92
–	10	–	0.076±0.009 (76.1±3.9)	36.8±5.1	0.372	–3.13±1.88
100	–	95±0.1 (95±1.2)	–	24±1.9	0.132	–3.55±0.65
200	–	187±0.5 (93.5±4)	–	26.5±3.2	0.222	–4.12±1.01
100	4	93.1±1.5 (93.1±1.92)	3.8±0.7 (95±2.4)	29.4±3.8	0.185	–3.63±0.69
200	4	149±12 (74.8±2.1)	3.6±0.3 (89.8±1.5)	34±4.9	0.276	–5.06±1.4
100	6	88.2±1 (88.2±1.1)	5±0.2 (83.3±1.7)	32.7±3.1	0.251	–2.76±1.44
200	6	131±0.7 (65.3±3.1)	3.3±0.6 (54.9±2.7)	40.1±3.5	0.343	–6.08±2.1
100	10	88.2±0.1 (88.2±2.3)	7.8±0.9 (78.2±1.5)	43±5.5	0.281	–3.88±0.64

Notes: [a]Actual loading expressed as amount (μg) of drug encapsulated per 10 mg of poloxamer; [b]EE% = ratio between experimental and theoretical loading ×100. Total of 10 mg, where 6.67 mg of P23 and 3.33 mg of F127. Results reported as mean values of three separated measurements on three different batches (n=9) ± standard deviation; –, The corresponding drug has not been included in the formulation.

Abbreviations: SRB, sorafenib; VP, verteporfin; EE, encapsulation efficiency; D_H, hydrodynamic diameter; PI, polydispersity index.

the product stored for 6 months. The high recovery yield observed highlighted that neither drug nor micelle precipitation occurred during the preparation.

Spectroscopic and photodynamic properties

Figure 1 shows the absorption and emission spectra of VP free and loaded in the micelles under various experimental conditions. VP is poorly soluble in water media, where it is mostly present as aggregated and nonfluorescent form (a and e in Figure 1). In contrast, poloxamer mixed micelles are able to entrap VP in the monomeric form, as confirmed by the sharpening of VP absorption bands and the intense fluorescence emission (b and f in Figure 1), similarly to VP in methanol, where it is present as monomer (d and h in Figure 1). Coentrapment of SRB and VP did not influence the absorption or emission behavior of the latter (c and g in Figure 1). In fact, only negligible changes were observed in the absorption region beyond 330 nm, being the SRB absorption dominating below this region. In addition, fluorescence emission was not affected either, being the fluorescence quantum yield ~0.06, basically the same value observed in methanol (Φ_F =0.051).[30]

The excited triplet state of the PS is the key transient intermediate for the photosensitization of $^1O_2$, and its effective generation is thus crucial for the photodynamic action.[31] Laser-flash photolysis with nanosecond time resolution is a powerful tool for obtaining spectroscopic and kinetic features of excited triplets of PS for PDT, since these transient species exhibit very intense absorptions in the visible region and possess lifetimes falling in the microsecond time regime.[32] Figure 2A shows the transient absorption spectra recorded at different delay times with respect to 532 nm laser excitation of poloxamer micelles coloaded with VP and SRB. The transient spectrum observed 0.8 μs after the pulse shows the typical features of the excited triplet state of the VP, with a maximum at ~480 nm and bleaching due to the ground-state absorption at ~400 nm.[33] The time evolution reveals that no new transient species was formed concurrently with the triplet decay. The triplet state decayed monoexponentially, with a triplet lifetime of ~15 μs, which matched the full recovery of the bleaching well (inset in Figure 2A). This spectroscopic and kinetic scenario is similar to that observed in the absence of SRB (data not shown), confirming that VP does not participate in any bimolecular process with the coencapsulated chemotherapeutic.

In order to gain insights into the efficiency of the population of the triplet state, we measured the laser-intensity dependence of transient absorbance under different experimental conditions. Figure 2B shows the top ΔA of the triplet absorption observed for VP incorporated in the micelles in the absence and in the presence of SRB, and (for comparison) for VP in methanol. The behavior observed was typical of a one-photon process, such as the generation of the lowest excited triplet state. In this case, the initial part of each set of data points is proportional to the product $\Phi_T \times \varepsilon_{T-T}$, where Φ_T and ε_{T-T} are the quantum yield of the triplet state and its molar absorption coefficient, respectively.

By taking into account the fact that all solutions were almost optically matched at the excitation wavelength (only slight differences in the absorption at 532 nm were observed in the whole range of ratios explored) and that

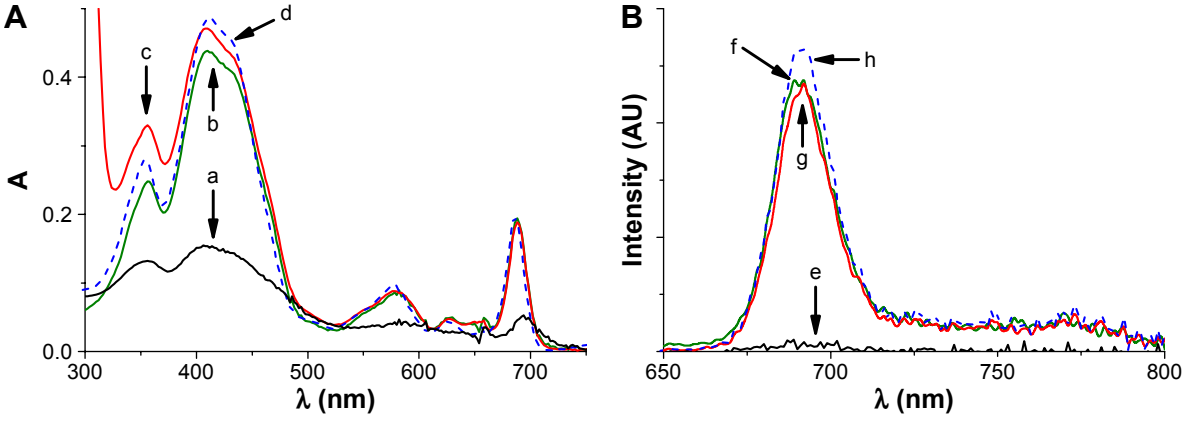

Figure 1 Absorption and emission spectra of VP in different media.
Notes: (**A**) Absorption spectra of VP in water (a), methanol (d), and in Pluronic® (poloxamer) P123/F127 mixed micelles (10 mg) dispersed in water solution in the absence (b) and in the presence of SRB (c). (**B**) Fluorescence-emission spectra (λ_{exc} =580 nm) of VP in water (e), methanol (h), and poloxamer micelles dispersed in water solution in the absence (f) and presence of SRB (g). VP and SRB concentrations were 4 and 100 μg·mL^{-1}, respectively.
Abbreviations: A, absorption; VP, verteporfin; SRB, sorafenib.

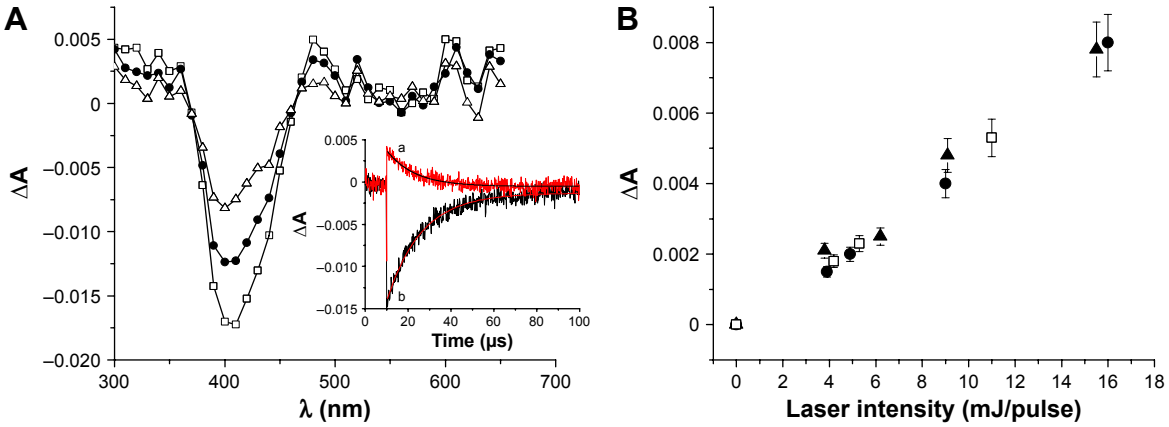

Figure 2 Triplet-state features of VP in different conditions.

Notes: (**A**) Transient absorption spectra observed 0.8 μs (□), 3.8 μs (●), and 8.7 μs (△) after 532 nm laser excitation (E_{532} ~10 mJ/pulse) of Ar-saturated, aqueous solution of Pluronic® (poloxamer) micelles coloaded with VP and SRB. The inset shows the decay trace monitored at 480 nm (a) and 400 nm (b) and the related first-order fittings. (**B**) Laser-intensity dependence of ΔA at 480 nm taken 0.1 μs after the laser pulse for VP in methanol (●) and in poloxamer micelles dispersed in water solution in the absence (▲) and presence (□) of SRB. VP and SRB concentrations were 4 and 100 μg·mL^{-1}, respectively.

Abbreviations: A, absorption; VP, verteporfin; SRB, sorafenib.

large changes in ε_{T-T} are fairly unlikely, as the band profiles were substantially unchanged, the very similar set of points obtained suggests that the efficiency of the population of the triplet state of VP in the poloxamer micelles was not affected by the presence of SRB and was very close to that observed in the methanol solution.

Energy transfer from the triplet of VP to molecular oxygen results in the concomitant photogeneration of $^1O_2$. Near-infrared luminescence is the most suitable technique to demonstrate unequivocally the generation of $^1O_2$. This species, in fact, exhibits a typical phosphorescence signal, with maximum at 1,270 nm.[34] Figure 3 shows the diagnostic phosphorescence spectrum for the poloxamer micelles loaded with VP alone and in the presence of SRB in D_2O solutions, this solvent being used to take advantage of the larger radiation constant and longer lifetime with respect to H_2O. Since all solutions are optically matched at the excitation wavelength, the very similar area of the spectra obtained for micelles containing either VP or VP coencapsulated with SRB lead us to conclude that the $^1O_2$ quantum yield of the PS is basically independent of the presence of the chemotherapeutic, according to what was observed for the precursor excited triplet state.

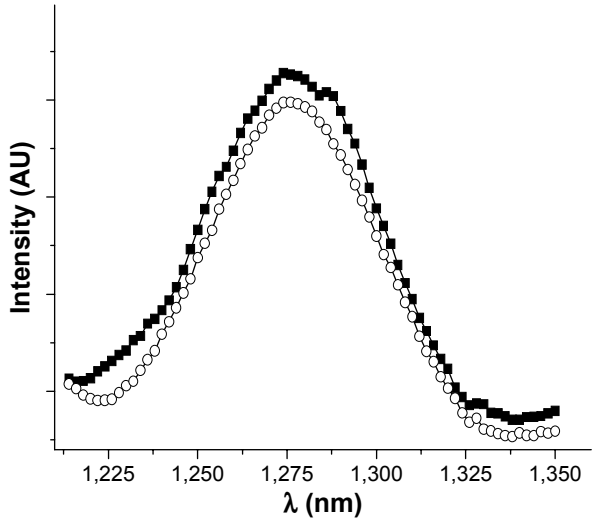

Figure 3 Singlet oxygen luminescence detected in D_2O solutions of Pluronic® (poloxamer) micelles loaded with VP in the absence (■) and in the presence (○) of SRB. λ_{exc} =405 nm.

Abbreviations: VP, verteporfin; SRB, sorafenib.

Micelle behavior in cell-culture medium

Interaction of micelles with proteins is regarded as a critical factor, since it has been demonstrated that micelles can aggregate/dissociate in complex media, altering the interpretation of biological results.[35] Therefore, the behavior of poloxamer micelles in DMEM enriched with 10% v:v of FBS was assessed by dynamic light-scattering (DLS) and fluorescence measurements. However, monitoring only one fluorescent probe in the medium can lead to a false-positive result, because even if the micelle is disrupted, the fluorescent tag could bind to FBS proteins, resulting in no significant change in fluorescence properties, as demonstrated for VP.[36] FRET represents an efficient tool to track nanoparticle stability in biologically relevant media.[27,37] For FRET evaluation, it was necessary to coencapsulate into the micelle core two fluorescent probes – an energy donor and an energy acceptor – with appropriate spectroscopic characteristics. The acceptor molecule in this work was VP. As donor, we chose the hydrophobic dye NR, since its emission spectrum

overlaps well with the VP-absorption spectrum, one of the indispensable requisites for FRET to be observed (Figure S2). NR presented a strong association constant with poloxamer micelles, and was located inside the poloxamer hydrophobic core. DLS measurements showed no significant change in size or ζ-potential after coencapsulation of VP and NR under the present conditions (data not shown).

Excitation at 480 nm of the micelle systems coencapsulating the two chromofluorogenic components and dispersed in cell-culture medium showed that the emission of the VP (λ_{em} =690 nm) dominated over the emission of the NR (λ_{em} =580 nm), despite NR absorbing most of the incident light and its fluorescence quantum yield being higher than that of VP (Figure 4A). The intense fluorescence of VP (less fluorescent probe) demonstrates that efficient energy transfer occurred, due to the close proximity of the coencapsulated molecules.

Solubilizing the same formulation in organic solvents disrupted its core–shell structure, releasing the fluorophores to the external medium. This led to an increase in the distance between the molecules and thus a dramatic reduction in FRET efficiency ($I_{690/580}$ reduced from 2.4 to 0.15, Figure 4A). Similar results were observed when the dyes were solubilized directly in cell-culture medium without micelles. This design allows the monitoring of micelle stability in different conditions.[27] No significant difference in FRET signal or size were observed for up to 72 hours for poloxamer mixed micelles incubated in cell-culture medium (Figure 4B), suggesting that the steric hindrance conferred by the PEO corona offered efficient protection against protein adsorption on the micelle surface and following disassembly.[38]

The release profile of dual-drug-loaded poloxamer mixed micelles dispersed in PBS at pH 7.4 and 37°C was evaluated by dialysis (Figure 5). Polysorbate 80 in the external medium ensured both sink conditions and prevention of drug aggregation. SRB–VP-loaded micelles displayed a lower rate of release compared to free SRB and VP (Figure 5A). The incomplete release of free VP was likely due to extensive aggregation in water, which hindered transport through the dialysis membrane. Since the amount of drug free to diffuse through cell membranes cannot be derived directly from release studies in PBS,[39]

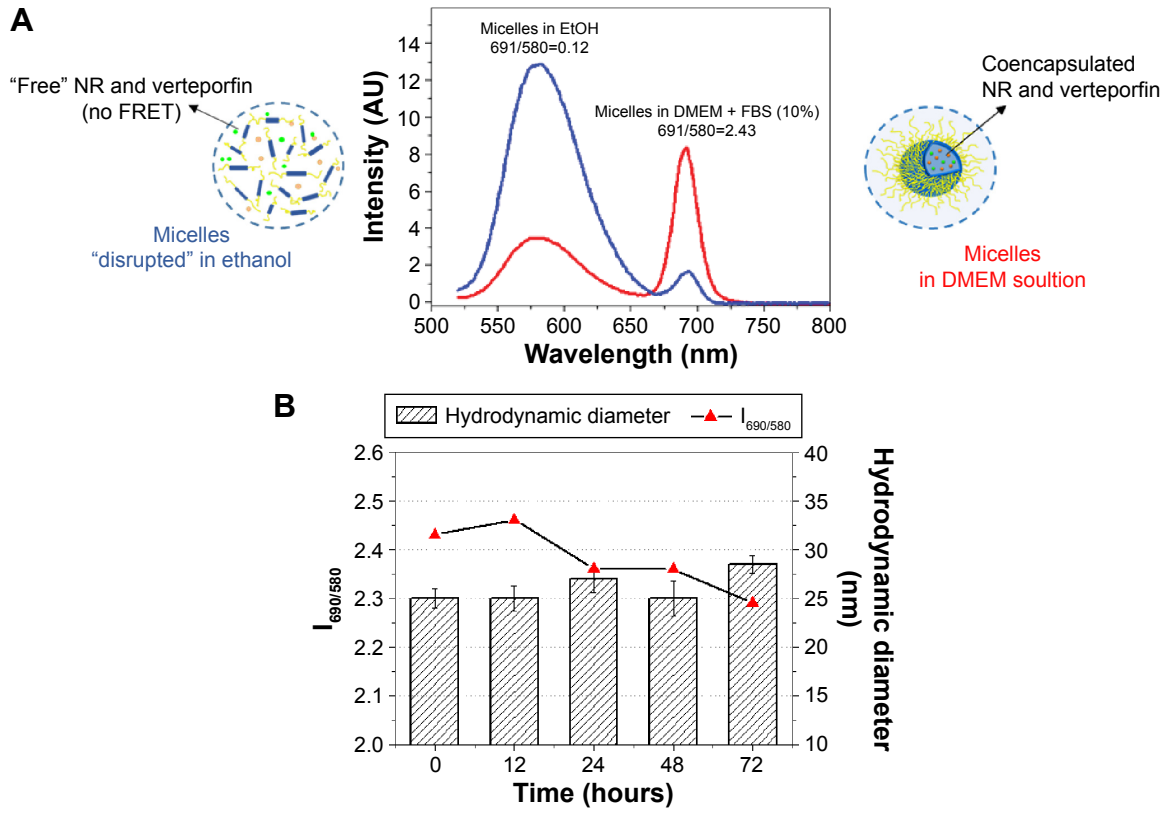

Figure 4 Behavior of Pluronic® (poloxamer) P123/F127 mixed micelles (10 mg) loaded with NR (0.8 μg·mL^{-1}) and VP (4.0 μg·mL^{-1}) in DMEM enriched with FBS 10% (v:v).
Notes: (**A**) Fluorescence-emission spectra of coencapsulated dyes in DMEM (red line) and diluted in ethanol (blue line) at λ_{exc} =480 nm. (**B**) Hydrodynamic diameter (bars) and fluorescence-intensity ratio between VP emission at 690 nm and NR emission at 580 nm (symbols). Data reported as mean values of three independent experiments (n=3) ± standard deviation.
Abbreviations: NR, Nile red; VP, verteporfin; DMEM, Dulbecco's Modified Eagle's Medium; FBS, fetal bovine serum; FRET, fluorescence resonance energy transfer; $I_{690/580}$, intensity ratio between emission at 690 and 580 nm.

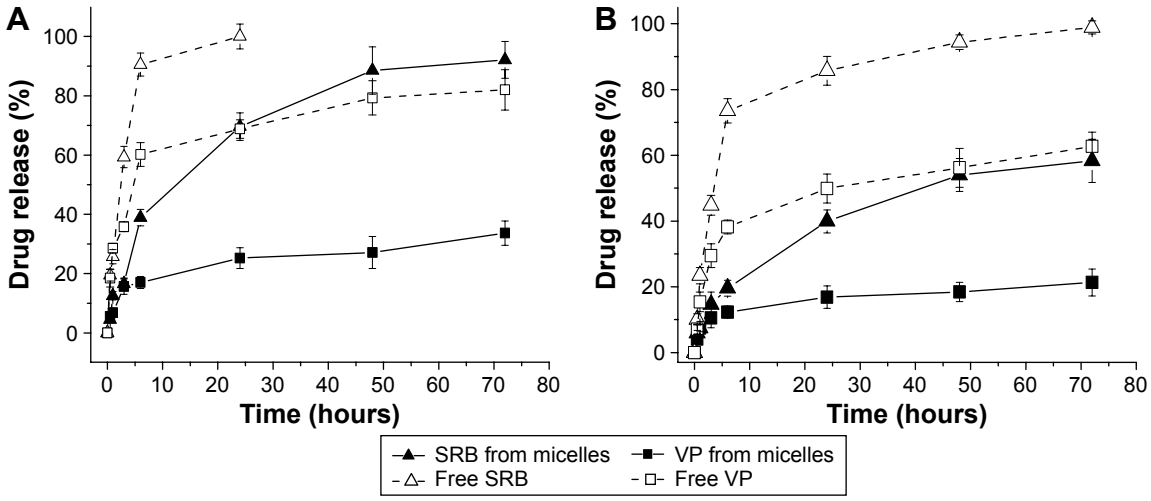

Figure 5 Release profile of SRB and VP as free or loaded in SRB/VP Pluronic® (poloxamer) P123/F127 micelles dispersed in (**A**) PBS or (**B**) DMEM with FBS 10%.
Notes: The external medium used for dialysis was PBS buffer with polysorbate 80 (5% v:v) at pH 7.4 and 37°C. SRB and VP concentrations were 100 and 10 μg·mL^{-1}, respectively. Data reported as mean values of three independent experiments (n=3) ± standard deviation.
Abbreviations: VP, verteporfin; SRB, sorafenib; PBS, phosphate-buffered saline; DMEM, Dulbecco's Modified Eagle's Medium; FBS, fetal bovine serum.

the release behavior was followed after micelle dispersion in DMEM enriched with FBS 10% v:v (Figure 5B). SRB presented a sustained released pattern, while VP remained substantially entrapped in the micelle core. Similarly to PBS, SRB–VP-loaded micelles displayed a lower rate of release compared to free SRB and VP. Furthermore, release in DMEM with FBS occurred at slower rates than in PBS (Figures 5, S3, and S4). Once it is assumed that micelles are stable in DMEM, as demonstrated by FRET, the interaction of SRB and VP with FBS proteins, especially albumin,[36] likely contributes to a decreased release rate. This hypothesis is supported by the fact that the release rate of free drug in DMEM is slower compared to PBS. Therefore, the fraction of drugs released from micelles can interact with medium proteins, contributing to albumin-mediated transport inside cells.[40]

The release profile from SRB–VP-loaded micelles in all the media was faster than that from micelles loaded with a single drug (Figures S3 and S4). This result, together with the slight increase micelle size when both drugs were coloaded, is indicative of the looser packing of hydrophobic PPO chains, which can lead to a faster release rate.

Cytotoxicity of SRB

The concentration-dependent cytotoxicity of SRB loaded in poloxamer micelles was measured in MDA-MB231 cells after 24 hours of exposure and compared to that of the free drug. Cell death measured with the MTS assay immediately after drug exposure was significantly higher for free SRB incubated at 15 or 20 μM with respect to SRB micelles, which in contrast demonstrated higher efficacy only at very low drug concentration (ie, 1 μM) (Figure 6A). However, the cytotoxicity of SRB delivered in poloxamer micelles was significantly higher with respect to free SRB 24 hours after drug exposure (24+24 hours), with half-maximal inhibitory concentration of 7.7 and 14.8 μM for SRB micelles and free SRB, respectively. The data suggest that after the removal of free SRB, the cells resumed proliferating, at least in the lower range of concentrations used in these experiments, while SRB in micelles exerted a delayed but stronger and prolonged cytotoxic effect that might be associated with slow but sustained release of the drug from micelles. Accordingly, free SRB did not perturb to a great extent the progression through the various phases of the cell cycle, nor did it cause the appearance of a hypodiploid cell population indicative of apoptosis (Figure 6B and C). On the contrary, SRB in poloxamer mixed micelles caused an accumulation of the cells in the S phase already at 24 hours, with a further increase at 24+24 hours (Figure 6C) and the appearance of hypodiploid events in the flow-cytometry histograms relative to cell DNA content (Figure 6B).

In any case, the induction of an apoptotic response was not ascribable to the presence of the delivery system, since empty poloxamer mixed micelles did not induce cytotoxicity or cell-cycle alterations in the same concentration range of SRB micelles (data not shown). Similarly to our results with MDA-MB231 cells, the induction of apoptosis was reported also for BGC-823 gastric cancer cells after incubation with SRB loaded in salicylic acid–chitosan/heparin-coated poloxamer nanoparticles.[41]

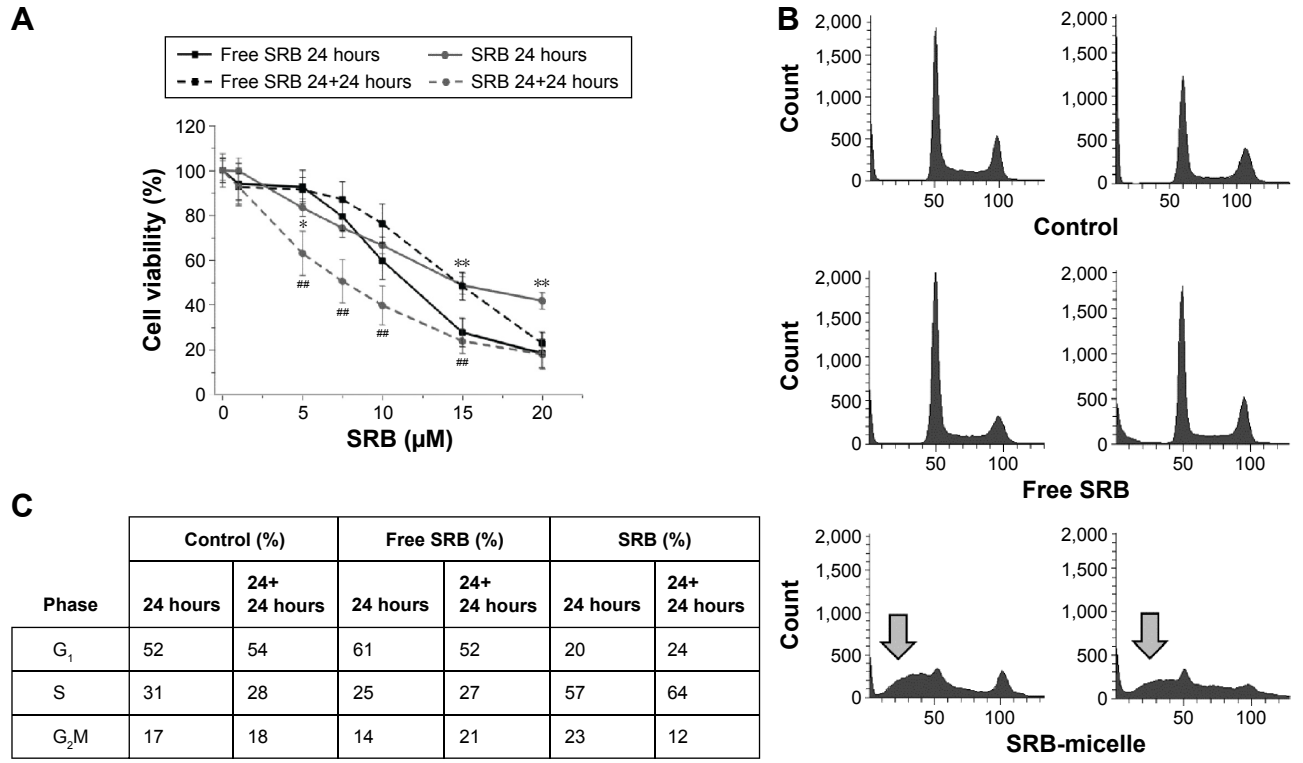

C

Phase	Control (%)		Free SRB (%)		SRB (%)	
	24 hours	24+ 24 hours	24 hours	24+ 24 hours	24 hours	24+ 24 hours
G_1	52	54	61	52	20	24
S	31	28	25	27	57	64
G_2M	17	18	14	21	23	12

Figure 6 Cytotoxicity of SRB-loaded Pluronic® (poloxamer) P123/F127 mixed micelles vs free SRB.
Notes: (**A**) Cell viability measured with the MTS assay in MDA-MB231 cells incubated with increasing concentrations of SRB free or loaded in micelles for 24 or 24+24 hours. Data are mean values ± standard deviation of at least three independent experiments carried out in triplicate. *$P<0.05$, **$P<0.001$ SRB micelles vs free SRB 24 hours; ##$P<0.001$ SRB micelles vs free SRB 24+24 hours (Student's *t*-test). (**B**) Representative cell-cycle histograms showing the appearance of a hypodiploid populations (gray arrows) in the samples treated with SRB micelles. (**C**) Summary of cell-cycle analysis.
Abbreviations: SRB, sorafenib; MTS, 3-(4,5-dimethylthiazol-2-yl)-5-(3-carboxymethoxyphenyl)-2-(4-sulfophenyl)-2*H*-tetrazolium.

Cytotoxicity of the combination SRB plus VP-mediated PDT

Based on the results reported, showing a benefit by delivering SRB in poloxamer micelles, and those reported previously by our group[7] on the delivery with the same micelles of the PS VP, we investigated the possibility of further improving the cytotoxic effect on MDA-MB231 cells by treating them with the combination of SRB and PDT with VP. Figure 7 shows that the reduction in viability of cells treated with PDT (irradiated with 0.75 J·cm^{-2} of red light) after 24 hours' incubation with the combination of free SRB + free VP was very similar to that measured after cell incubation and irradiation with free VP only. The absence of any increased cytotoxicity of the combination with respect to free VP alone is very likely explained by the negligible cytotoxicity of free SRB at 24+24 hours (Figure 6), ie, the same time point at which the viability of PDT-treated cells was measured.

The experiments with the combination in the dark confirmed that free SRB was poorly cytotoxic at concentrations lower than 10 μM (Figure S5). These latter experiments also confirmed that VP alone was devoid of any toxicity in the absence of light, independently of delivery modality.

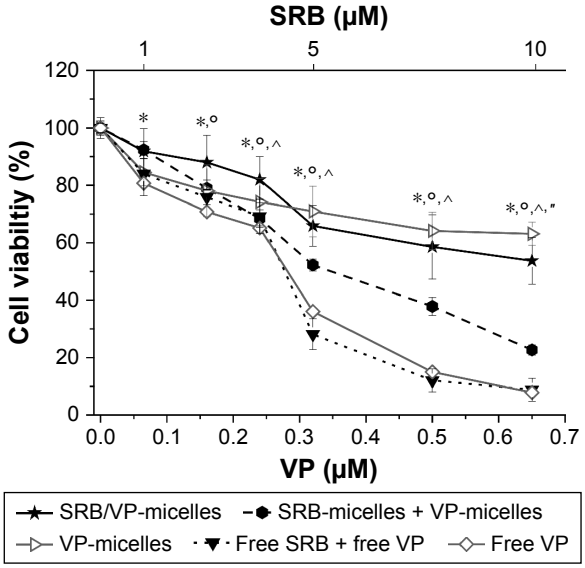

Figure 7 Phototoxicity in MDA-MB231 cells.
Notes: Cells exposed to the photosensitizer alone (VP) or to the drug combination (VP + SRB) delivered or not by Pluronic® (poloxamer) P123/F137 micelles (24 hours) and irradiated with 0.75 J·cm^{-2} of red light. Cell viability was measured with MTS assay at 24 hours postirradiation. Data are mean values ± standard deviation of at least three independent experiments carried out in triplicate. Bonferroni test ($P<0.05$): SRB/VP micelles significantly different from *free VP, °free SRB + free VP, ^VP micelles + SRB micelles, "VP micelles.
Abbreviations: VP, verteporfin; SRB, sorafenib; MTS, 3-(4,5-dimethylthiazol-2-yl)-5-(3-carboxymethoxyphenyl)-2-(4-sulfophenyl)-2*H*-tetrazolium.

Contrary to our expectation, the combination of SRB and VP formulated in separate micelles was less phototoxic than the combination of the free drugs. This was very likely caused by the reduced phototoxicity of VP-loaded micelles in comparison to free VP. In any case, the treatment with the combination of VP poloxamer-mediated PDT and SRB-loaded micelles was slightly more efficient in reducing cell viability than the single treatments. This positive interaction, though, appeared disturbed by the encapsulation of the two drugs in the same micelles for their codelivery to MDA-MB231 cells. In fact, the reduction in viability in cells treated with VP–SRB-loaded poloxamer micelles was less than that caused by VP micelles plus SRB micelles added separately. One possible explanation for the reduced efficacy of the combination of coloaded VP–SRB is the increased size of micelles associated with drug coencapsulation, as shown by the DLS measurements of Table 1, which might have reduced the efficiency of cell internalization and drug bioavailability.

Uptake and cellular localization of benzoporphyrin-derivative monoacid ring A in MDA-MB231 cells

The hypothesis of a reduced cellular uptake of drugs encapsulated in micelles compared to the free forms was confirmed for VP. The red fluorescence of VP was exploited to investigate easily both the cellular uptake by flow cytometry and cellular localization by confocal microscopy. We found that the uptake of free VP in MDA-MB231 cells incubated for 24 hours increased linearly at least up to 1.5 µM (Figure 8A).

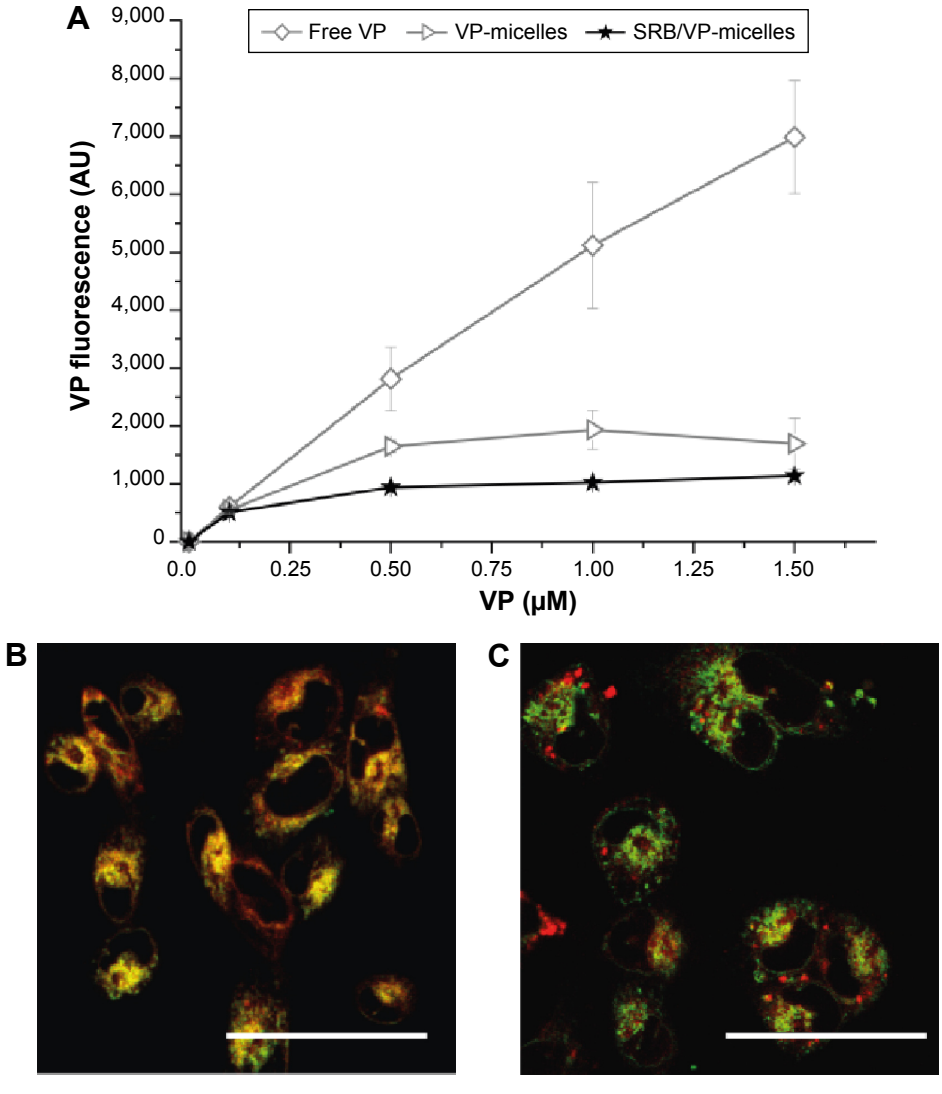

Figure 8 Uptake and intracellular localization of VP formulations.
Notes: (**A**) Flow-cytometry measurements of VP uptake after 24 hours of cell incubation with increasing concentrations of free VP, VP micelles, or VP/SRB micelles. Confocal microscopy images of MDA-MB231 cells incubated with free (**B**) or VP-loaded (**C**) micelles (red fluorescence) for 24 hours and stained with the endoplasmic reticulum probe ER-Tracker green (green fluorescence). Clear colocalization between the probe and VP fluorescence is visible exclusively in (**B**). Scale bar: 50 µm.
Abbreviations: VP, verteporfin; SRB, sorafenib.

On the contrary, the uptake of VP loaded in poloxamer micelles reached a plateau at approximately 0.5 μM. Of interest is the fact that coloaded VP–SRB micelles showed a decreased uptake at the plateau with respect to VP-loaded micelles.

Note that the reduced cellular uptake of the micelles cannot be trivially ascribed to lower fluorescence of the VP when encapsulated in the carrier. In fact, we demonstrated that the fluorescence quantum yield of this fluorophore was not affected by its compartmentalization in the poloxamer micelles, and was also independent of the presence of SRB. Therefore, reduced uptake of VP when loaded in micelles parallels the poor internalization of PEO-coated nanocarriers.[42] The observations on the decreasing uptake of VP well correlate with the decrease in cell photosensitization efficiency, which was higher for free VP with respect to VP-loaded micelles (Figure 7). For VP–SRB-loaded micelles, we can safely assume that based on the uptake experiments, the contribution of PDT to the overall effect of the combined treatment is less than in the combination VP-loaded micelles + SRB-loaded micelles, with consequent decreased cell mortality. The fluorescence-microscopy analyses (Figure 8B and C) confirmed the lower uptake of VP-loaded micelles with respect to free VP, and showed cytoplasmic localization of both formulations, with exclusive accumulation of free VP in the endoplasmic reticulum.

Moreover, together with the reduced uptake, the different intracellular localization of the two formulations could have been responsible for the reduced phototoxic profile measured for VP-loaded micelles, at least in MDA-MB 231 cells. In our previous work, we reported a mitochondrial localization of both free and micelle VP in HeLa cells and significantly increased phototoxicity of VP with delivery by poloxamer micelles for PS concentrations lower than 0.1 μM.[7] It must, however, be considered that the latter results were obtained in HeLa cells incubated with VP for 4 hours only before performing PDT. Therefore, to exclude any timing effects that might negatively affect cell-photosensitization and/or drug-combination sequence, we performed experiments in which MDA-MB231 cells were incubated for 4 hours with VP, irradiated with 0.75 $J \cdot cm^{-2}$ of red light, and incubated for a further 24 hours with SRB (Figure S6). The changing incubation time and schedule of delivery of the treatments, however, did not improve the cytotoxic effects of the combination of VP PDT and SRB, and did not show any synergism or additive effects for the drugs delivered free or in poloxamer mixed micelles.

Conclusion

The present study demonstrates that poloxamer mixed micelles do not suffer disassembly or size changes in biological media, and are very suited to entrap effectively the poorly water soluble SRB, VP, and their combination. While the cytotoxicity of SRB delivered by poloxamer micelles was significantly higher than that observed for the free drug, the effect was the opposite for VP. Furthermore, micelles codelivering the two active components did not improve anticancer performance. These findings cannot be attributable to reduced photodynamic properties of VP when encapsulated in the micelles, being its capability to photogenerate $^1O_2$ basically the same as that observed in organic solvent and in the micelles coencapsulating SRB. One possible explanation of the reduced efficacy of the VP–SRB combination is the different cell uptake and localization of the micelles, which resulted in reduced efficiency of cell internalization and drug bioavailability. In view of previous research reporting enhanced cytotoxic effects on systems based on photochemotherapeutic combination, the present contribution provides a clear example that no generalizations are possible in this regard, and that each system must be investigated in detail. Coencapsulation of a PDT agent and a chemotherapeutic in a single nanodelivery system cannot be proposed as a general strategy to observe amplified cell-mortality effects, even under the complete preservation of the photodynamic properties of the PS in the copresence of the chemotherapeutic agent, which in any case remain always a key prerequisite to be fulfilled.

Acknowledgments

FQ wishes to thank the Italian Ministry of University and Research (PRIN 2010H834LS) and Italian Association for Cancer Research (IG2014, for 15764) for financial support. SS thanks PON Hippocrates (2013–2015) for financial support. DSP and NH wish to thank the Brazilian agency Coordenação de Aperfeiçoamento de Pessoal de Nível Superior (CAPES), process number BEX 14036/13-14.

Disclosure

The authors report no conflicts of interest in this work.

References

1. Aw MS, Kurian M, Losic D. Polymeric micelles for multidrug delivery and combination therapy. *Chemistry*. 2013;19:12586–12601.
2. Sanna V, Pala N, Sechi M. Targeted therapy using nanotechnology: focus on cancer. *Int J Nanomedicine*. 2014;9:467–483.
3. Xu X, Ho W, Zhang X, Bertrand N, Farokhzad O. Cancer nanomedicine: from targeted delivery to combination therapy. *Trends Mol Med*. 2015; 21:223–232.

4. Batrakova EV, Kabanov AV. Pluronic block copolymers: evolution of drug delivery concept from inert nanocarriers to biological response modifiers. *J Control Release*. 2008;130:98–106.
5. Jung YW, Lee H, Kim JY, Koo EJ, Oh KS, Yuk SH. Pluronic-based core/shell nanoparticles for drug delivery and diagnosis. *Curr Med Chem*. 2013;20:3488–3499.
6. Attia ABE, Ong ZY, Hedrick JL, et al. Mixed micelles self-assembled from block copolymers for drug delivery. *Curr Opin Colloid Interface Sci*. 2011;11:182–184.
7. Pellosi DS, Tessaro AL, Moret F, et al. Pluronic® mixed micelles as efficient nanocarriers for benzoporphyrin derivatives applied to photodynamic therapy in cancer cells. *J Photochem Photobiol A Chem*. 2016;314:143–154.
8. Wilhelm S, Carter C, Lynch M, et al. Discovery and development of sorafenib: a multikinase inhibitor for treating cancer. *Nat Rev Drug Discov*. 2006;5:835–844.
9. Bolondi L, Craxi A, Trevisani F, et al. Refining sorafenib therapy: lessons from clinical practice. *Future Oncol*. 2015;11:449–465.
10. Lin T, Gao DY, Liu YC, et al. Development and characterization of sorafenib-loaded PLGA nanoparticles for the systemic treatment of liver fibrosis. *J Control Release*. 2016;221:62–70.
11. Craparo EF, Sardo C, Serio R, et al. Galactosylated polymeric carriers for liver targeting of sorafenib. *Int J Pharm*. 2014;466:172–180.
12. Bondi ML, Botto C, Amore E, et al. Lipid nanocarriers containing sorafenib inhibit colonies formation in human hepatocarcinoma cells. *Int J Pharm*. 2015;493:75–85.
13. Thapa RK, Choi JY, Poudel BK, et al. Multilayer-coated liquid crystalline nanoparticles for effective sorafenib delivery to hepatocellular carcinoma. *ACS Appl Mater Interfaces*. 2015;7:20360–20368.
14. Xie B, Wang DH, Spechler SJ. Sorafenib for treatment of hepatocellular carcinoma: a systematic review. *Dig Dis Sci*. 2012;57:1122–1129.
15. Weiss A, den Bergh H, Griffioen AW, Nowak-Sliwinska P. Angiogenesis inhibition for the improvement of photodynamic therapy: the revival of a promising idea. *Biochim Biophys Acta*. 2012;1826:53–70.
16. Dolmans DE, Fukumura D, Jain RK. Photodynamic therapy for cancer. *Nat Rev Cancer*. 2003;3:380–387.
17. Lucky SS, Soo KC, Zhang Y. Nanoparticles in photodynamic therapy. *Chem Rev*. 2015;115:1990–2042.
18. Huggett MT, Jermyn M, Gillams A, et al. Phase I/II study of verteporfin photodynamic therapy in locally advanced pancreatic cancer. *Br J Cancer*. 2014;110:1698–1704.
19. Nowak-Sliwinska P, Weiss A, van Beijnum JR, et al. Angiostatic kinase inhibitors to sustain photodynamic angio-occlusion. *J Cell Mol Med*. 2012;16:1553–1562.
20. Bennet D, Marimuthu M, Kim S, An J. Dual drug-loaded nanoparticles on self-integrated scaffold for controlled delivery. *Int J Nanomedicine*. 2012;7:3399–3419.
21. Mignani S, Bryszewska M, Klajnert-Maculewicz B, Zablocka M, Majoral JP. Advances in combination therapies based on nanoparticles for efficacious cancer treatment: an analytical report. *Biomacromolecules*. 2015;16:1–27.
22. Batist G, Gelmon KA, Chi KN, et al. Safety, pharmacokinetics, and efficacy of CPX-1 liposome injection in patients with advanced solid tumors. *Clin Cancer Res*. 2009;15:692–700.
23. Feldman EJ, Lancet JE, Kolitz JE, et al. First-in-man study of CPX-351: a liposomal carrier containing cytarabine and daunorubicin in a fixed 5:1 molar ratio for the treatment of relapsed and refractory acute myeloid leukemia. *J Clin Oncol*. 2011;29:979–985.
24. He C, Liu D, Lin W. Self-assembled core-shell nanoparticles for combined chemotherapy and photodynamic therapy of resistant head and neck cancers. *ACS Nano*. 2015;9:991–1003.
25. Maiolino S, Moret F, Conte C, et al. Hyaluronan-decorated polymer nanoparticles targeting the CD44 receptor for the combined photo/chemo-therapy of cancer. *Nanoscale*. 2015;7:5643–5653.
26. Zhang X, Jackson JK, Burt HM. Development of amphiphilic diblock copolymers as micellar carriers of taxol. *Int J Pharm*. 1996;132:195–206.
27. Chen H, Kim S, He W, et al. Fast release of lipophilic agents from circulating PEG-PDLLA micelles revealed by in vivo Förster resonance energy transfer imaging. *Langmuir*. 2008;24:5213–5217.
28. Wei Z, Hao J, Yuan S, et al. Paclitaxel-loaded Pluronic P123/F127 mixed polymeric micelles: formulation, optimization and in vitro characterization. *Int J Pharm*. 2009;376:176–185.
29. Park S, Jeong K, Lee E, et al. Amphiphilized poly(ethyleneimine) nanoparticles: a versatile multi-cargo carrier with enhanced tumor-homing efficiency and biocompatibility. *J Mater Chem B Mater Biol Med*. 2015;3:198–206.
30. Aveline BM, Hasan T, Redmond RW. The effects of aggregation, protein binding and cellular incorporation on the photophysical properties of benzoporphyrin derivative monoacid ring A (BPDMA). *J Photochem Photobiol B*. 1995;30:161–169.
31. Kadish K, Smith KM, Guilard R, editors. *The Porphyrin Handbook*. San Diego: Academic Press; 2000.
32. Montalti M, Credi A, Prodi L, Gandolfi MT. *Handbook of Photochemistry*. 3rd ed. Boca Raton (FL): CRC Press; 2006.
33. Nowak-Sliwinska P, Karocki A, Elas M, Pawlak A, Stochel G, Urbanska K. Verteporfin, photofrin II, and merocyanine 540 as PDT photosensitizers against melanoma cells. *Biochem Biophys Res Commun*. 2006;349:549–555.
34. Wilkinson F, Helman WP, Ross AB. Quantum yields for the photosensitized formation of the lowest electronically excited singlet state of molecular oxygen in solution. *J Phys Chem Ref Data*. 1993;22:113–262.
35. Conte C, Ungaro F, Maglio G, et al. Biodegradable core-shell nanoassemblies for the delivery of docetaxel and Zn(II)-phthalocyanine inspired by combination therapy for cancer. *J Control Release*. 2013;167:40–52.
36. Chowdhary RK, Shariff I, Dolphin D. Drug release characteristics of lipid based benzoporphyrin derivative. *J Pharm Pharm Sci*. 2003;6:13–19.
37. Swaminathan S, Garcia-Amorós J, Fraix A, Kandoth N, Sortino S, Raymo FM. Photoresponsive polymer nanocarriers with multifunctional cargo. *Chem Soc Rev*. 2014;43:4167–4178.
38. Shubhra QT, Tóth J, Gyenis J, Feczkó T. Poloxamers for surface modification of hydrophobic drug carriers and their effects on drug delivery. *Polym Rev (Phila Pa)*. 2014;54:122–138.
39. Gullotti E, Yeo Y. Beyond the imaging: limitations of cellular uptake study in the evaluation of nanoparticles. *J Control Release*. 2012;164:170–176.
40. Palma G, Conte C, Barbieri A, et al. Antitumor activity of PEGylated biodegradable nanoparticles for sustained release of docetaxel in triple-negative breast cancer. *Int J Pharm*. 2014;473:55–63.
41. Yang YC, Cai J, Yin J, Zhang J, Wang KL, Zhang ZT. Heparin-functionalized Pluronic nanoparticles to enhance the antitumor efficacy of sorafenib in gastric cancers. *Carbohydr Polym*. 2016;136:782–790.
42. Conte C, d'Angelo I, Miro A, Ungaro F, Quaglia F. PEGylated polyester-based nanoncologicals. *Curr Top Med Chem*. 2014;14:1097–1114.

Supplementary materials

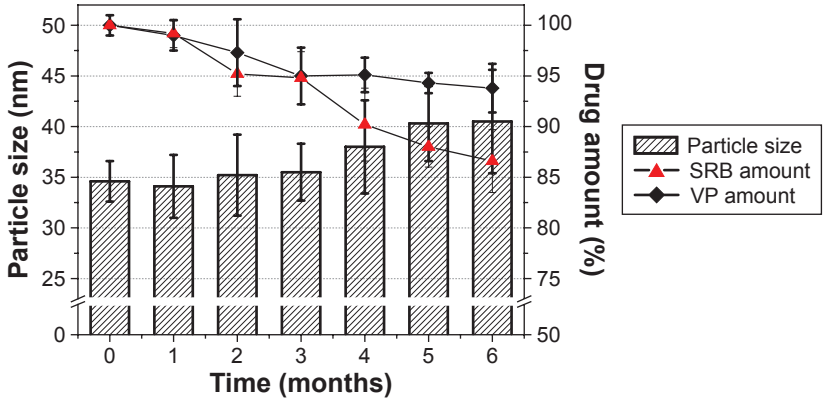

Figure S1 Storage stability of lyophilized Pluronic® P123/F127 mixed micelle formulations at room temperature.
Note: Results reported as mean values of three independent experiments (n=3) ± standard deviation.
Abbreviations: SRB, sorafenib; VP, verteporfin.

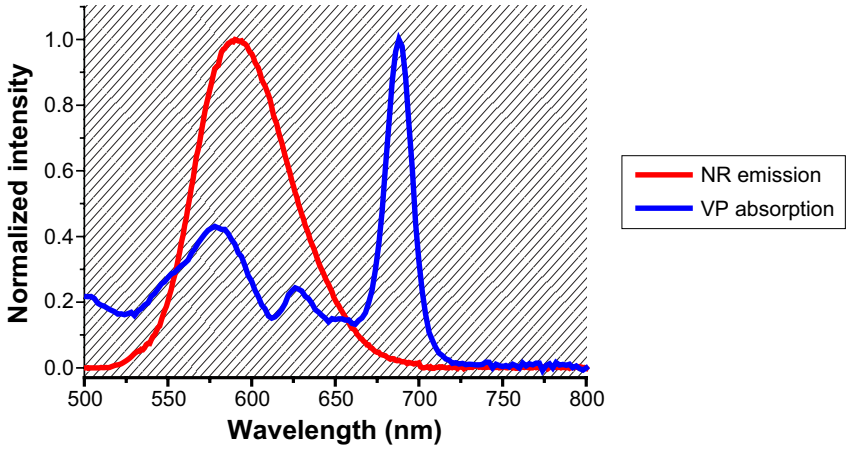

Figure S2 Absorption and emission spectra of VP and NR, respectively.
Notes: Normalized absorption spectrum of verteporfin (VP) and emission spectrum of Nile red (NR; λ_{exc} =480 nm) coloaded in Pluronic® P123/F127 mixed micelles dispersed in phosphate-buffered saline at pH 7.4 and 37°C. VP =4 μg·mL^{-1} and NR =0.8 μg·mL^{-1}. The shaded area represents the overlap of the evaluated spectra.

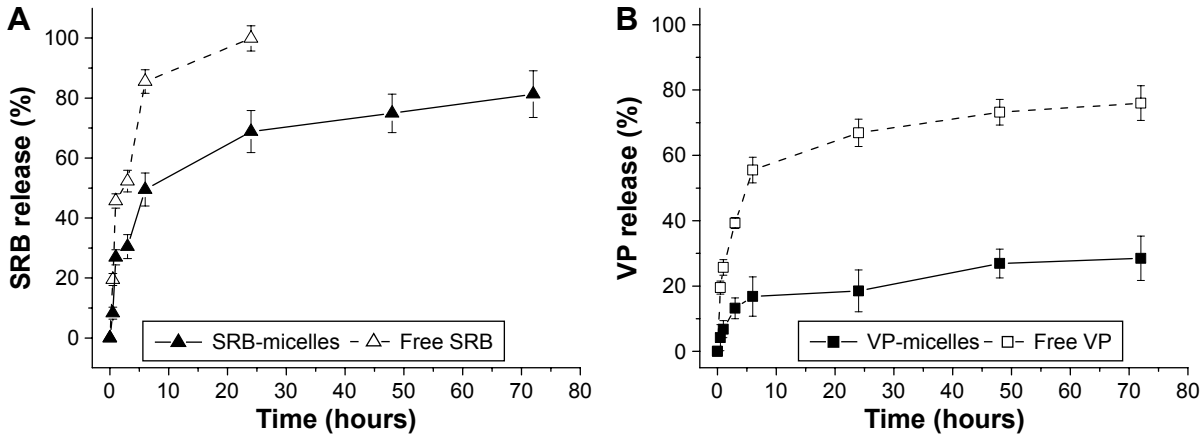

Figure S3 Release profile of free (**A**) SRB and (**B**) VP from Pluronic® P123/F127 mixed micelles in phosphate-buffered saline (PBS) at pH 7.4 and 37°C.
Notes: The external medium used for dialysis was PBS with polysorbate 80 (5% v:v) at pH 7.4 and 37°C. SRB =100 μg·mL^{-1} and VP =10 μg·mL^{-1}. Data reported as mean values of three independent experiments (n=3) ± standard deviation.
Abbreviations: SRB, sorafenib; VP, verteporfin.

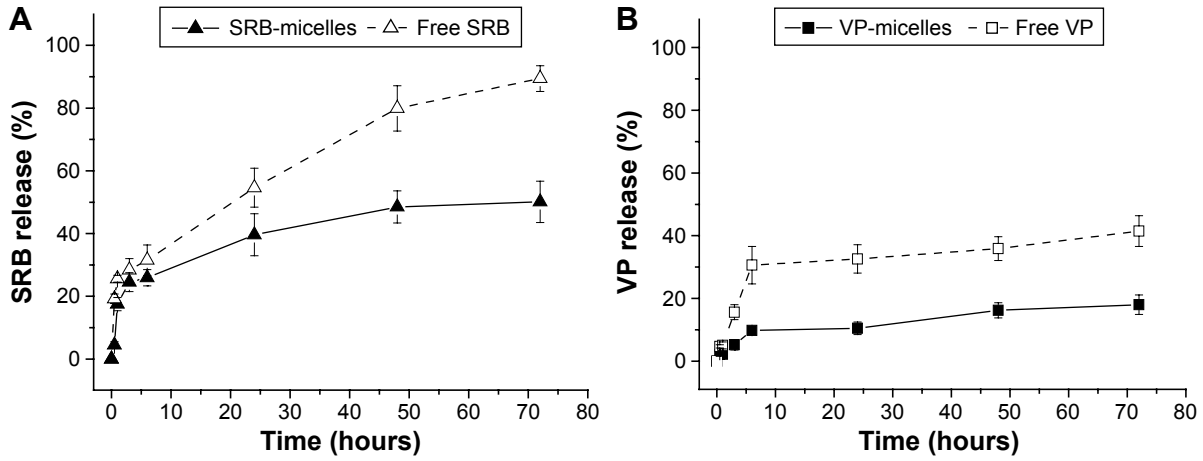

Figure S4 Release profile of (**A**) SRB and (**B**) VP from Pluronic® P123/F127 mixed micelles dispersed in DMEM enriched with FBS 10%.
Notes: Release profile of free and micelle-loaded (**A**) SRB and (**B**) VP from Pluronic® P123/F127 mixed micelles dispersed in DMEM enriched with FBS 10%. The external medium used for dialysis was phosphate-buffered saline with polysorbate 80 (5% v:v) at pH 7.4 and 37°C. SRB =100 μg·mL^{-1} and VP =10 μg·mL^{-1}. Data are reported as mean values of three independent experiments (n=3) ± standard deviation.
Abbreviations: SRB, sorafenib; VP, verteporfin; DMEM, Dulbecco's Modified Eagle's Medium; FBS, fetal bovine serum.

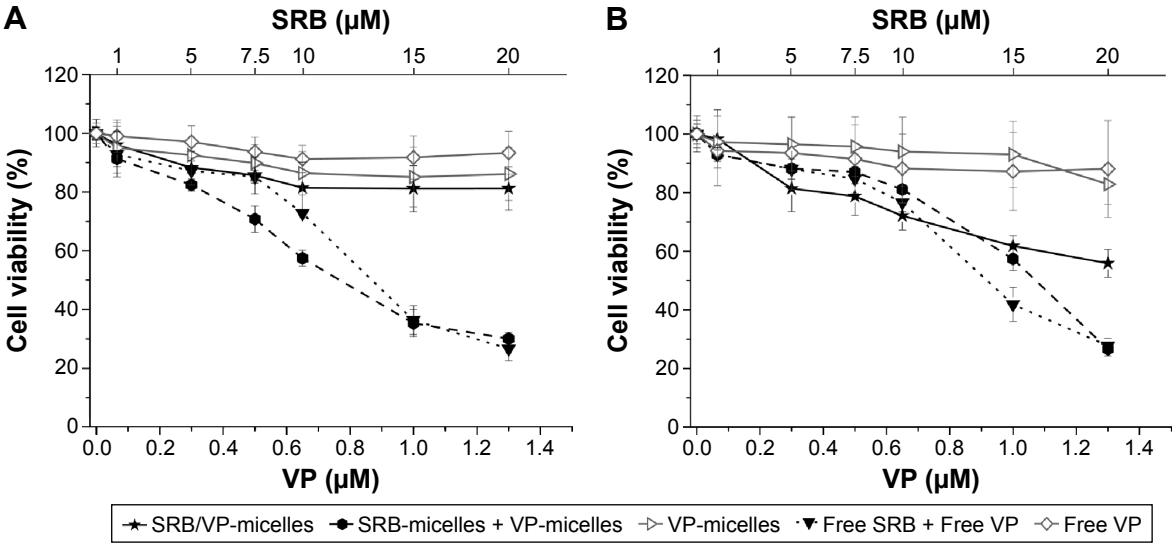

Figure S5 Dark cytotoxicity in MDA-MB231 cells.
Notes: Cells incubated in the dark with VP alone or to the drug combination (VP + SRB) delivered or not by Pluronic® P123/F137 mixed micelles for 24 hours (**A**) or 24+24 hours (**B**). Cell viability was measured at the end of incubation time with the MTS assay. Data reported as mean values of at least three independent experiments carried out in triplicate ± standard deviation.
Abbreviations: SRB, sorafenib; VP, verteporfin; MTS, 3-(4,5-dimethylthiazol-2-yl)-5-(3-carboxymethoxyphenyl)-2-(4-sulfophenyl)-2*H*-tetrazolium.

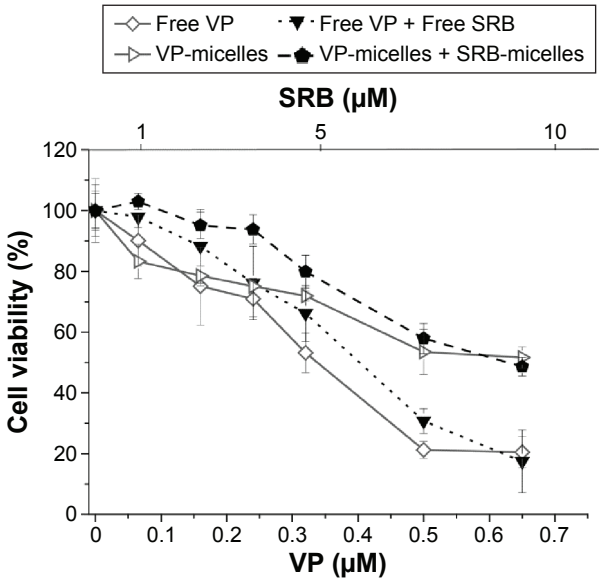

Figure S6 Cytotoxicity of MDA-MB231 cells incubated in the dark for 4 hours with VP (free or loaded in micelles) and irradiated with 0.75 J·cm^2 of red light.
Notes: Some samples were further incubated with SRB (free or loaded in micelles) for 24 hours. Cell viability was measured with the MTS assay at the end of SRB incubation or after 24 hours of cell release in VP-free medium for the samples not incubated with SRB. Data reported as mean values of at least two independent experiments carried out in triplicate ± standard deviation.
Abbreviations: SRB, sorafenib; VP, verteporfin; MTS, 3-(4,5-dimethylthiazol-2-yl)-5-(3-carboxymethoxyphenyl)-2-(4-sulfophenyl)-2*H*-tetrazolium.